AE-189
UDC 539.125.5.162.5
539.171.018

AE-189

An Electromagnet for Precession of the Polarization of Fast-Neutrons

O. Aspelund, J. Björkman and G. Trumpy

AKTIEBOLAGET ATOMENERGI

STOCKHOLM, SWEDEN 1965

AN ELECTROMAGNET FOR PRECESSION OF THE POLARIZATION OF FAST-NEUTRONS

O. Aspelund, J. Björkman and G. Trumpy [x]

Abstract

The advantages of using a transverse magnetic field for processing the polarization of fast-neutrons are discussed. Design details of a powerful electromagnet supplying a transverse field of approximately 20 kGauss are given. Precession characteristics for polarized fast-neutrons obtained at 50° (lab. syst.) from the $Li^7(p,n)Be^7$ reaction are reported, using elastic scattering at 42° (lab. syst.) off natural carbon as an analyser. Correlation of the precession data with theoretical predictions presented elsewhere is made, and good agreement is found.

[x] Now at Danmarks Tekniske Höjskole, Copenhagen, Denmark

Printed and distributed in May, 1965.

LIST OF CONTENTS

1. Introduction

Fast-neutron polarization experiments have lately become of considerable importance for unraveling the complexities of nuclear forces, and a number of such experiments have been reported (see ref. 1 for an extensive bibliography). The principle of a fast-neutron polarization experiment is depicted in fig. 1. Unpolarized charged-particles, e.g. protons, deuterons, or α-particles, are incident on a neutron-producing target. Generally, the emitted neutrons will be partially polarized with a polarization $\vec{P}_1 = \vec{P}_1(\theta_1)$ that is normal to the reaction plane. A part of the neutrons produced is collimated and elastically scattered off a scattering sample, and finally the scattered neutrons are detected by two identical detectors D_L and D_R. In general, these detectors will record different scattered intensities N_L and N_R resp.

In the idealized case of point target, point scatterer, and identical point detectors the following relation prevails (Basel convention)

$$P_1P_2 = P_1(\theta_1)\,P_2(\theta_2) = \frac{1 - N_L/N_R}{1 + N_L/N_R} \tag{1}$$

where P_2 is the polarization acquired by unpolarized neutrons if they were incident on the scattering sample. $\vec{P}_2$ is normal to the scattering plane. $\frac{N_L}{N_R}$ is the left-right intensity ratio. It is not feasible to design two detectors whose relative efficiencies are sufficiently well known for the faithful determination of the rather small intensity differences between these detectors without committing serious errors. The practical way of performing a polarization experiment is therefore to use one movable detector and successively record the scattered intensities in the left and right positions with respect to the incident fast-neutron beam. However, also this procedure is vulnerable to false asymmetries, which easily may mask the true asymmetries being looked for. Contributions to the false asymmetries may come from

1) mechanical deficiencies, namely

a) difficulties in attaining equality and reproducibility of the left and right detector positions

b) other mechanical short-comings of the experimental set-up

2) non-ideal neutron optical conditions caused by finite size of the beam profile, implying variations in neutron intensity, energy, and polarization across the scattering sample.

The ensuing systematic errors are considered in detail in ref. [2], where it is shown that by proper design of the mechanical details of the experimental set-up the false asymmetries under 1) may be kept under control. However, the systematic errors introduced by the finite beam profile are difficult to handle analytically, because for intensity reasons both the scattering sample and the detectors will have to be of considerable physical extension.

As first pointed out by Wilson [3a] the use of homogeneous magnetic fields will be of considerable advantage in alleviating the latter type of difficulties, because through the Larmor precession of the neutron polarization in the magnetic field the left-right ratio may be determined without performing an azimuthal displacement of the detector(s). This stems from the fact that only a microscopic property of the neutron beam (the magnetic moment of the separate neutron) is affected, whereas the macroscopic properties such as beam profile and position remain the same. Hillman and co-workers [3b] were the first to report on the sucessful application of a longitudinal magnetic field generated by a solenoid, in high energy neutron polarization experiments. Later, solenoids have found applications also in low energy neutron polarization work [4-8].

However, the design considerations preceding the fast-neutron polarization facility being operated in conjunction with the Studsvik 6 MeV Van de Graaff * (see below and also ref. 9) lead to the conclusion that the application of a transverse magnetic field between the neutron-producing target and the scattering sample would be particularly favourable.

---

* Type CN, delivered by High Voltage Engineering Corporation, Burlington, Massachusetts, U.S.A.

The large electromagnet subsequently designed generates a field of sufficient strength for precessing through 180° the polarization of fast-neutrons of energies up to approximately 10 MeV. Similar magnets were also constructed in other fast-neutron laboratories, and a few polarization data have been obtained by using these magnets [10-13]. So far, however, no separate descriptions of them have been published, and we therefore find it appropriate to describe our equipment somewhat more detailed than elsewhere done [xx].

2. Design considerations

As pointed out in refs. [2, 9, 15a and 15b] the fast-neutron polarization set-up is intended for

1) investigations of the partially polarized neutrons emanating from charged-particle reactions

2) studies of the polarization acquired by neutrons in elastic scattering from various nuclei.

Bearing this information in mind intensity considerations settled the following dimensions:

1) target-to-scatterer distance $\approx$ 100 cm
2) scatterer-to-detector distance $\approx$ 25 cm

One realizes that this compromise is compatible with the insertion of a comparatively large electromagnet between target and scatterer. Indeed, if a homogeneous field of about 19 kGauss is effective along a distance $\approx$ 40 cm this field will be sufficiently strong for precessing through 180° the polarization of neutrons of maximum energy $\approx$ 10 MeV. (See calculations in the Appendix). Also, because of the bulkiness of an electromagnet it will form an excellent fast-neutron and γ-ray shield.

The following considerations favoured the choice of a transverse magnetic field generated by an electromagnet:

[xx] Preliminary accounts of the design and the performance of the precession magnet are found in refs. [14a - 15b].

1) small power consumption

2) negligible stray magnetic fields

3) possibility of keeping reaction and scattering planes coplanar

4) possibility of measuring unpolarized differential scattering cross sections

5) possibility of designing the pole pieces of the electromagnet so that they form parts of the neutron collimator assembly.

As the precession of the magnetic moments of the neutrons takes place with the direction of the magnetic field as the precession axis (see fig. 2), the maximum field strength needed will be governed by the maximum energy of the neutrons whose magnetic moments are to be precessed through 180°. To some extent this requirement offsets the advantage of using an electromagnet whose power requirements are low, as compared to a solenoid where the maximum precession angles wanted are just $\pm 90^{\circ}$. However, practical reasons dictate the desirability of keeping reaction and scattering planes coplanar. Further, the stray magnetic fields of a solenoid are very troublesome to handle, whereas in the case of a properly designed electromagnet they will present no problems at all, leaving both the target spot and the sensitivity of the photo-multipliers unaffected.

It is clear that by precessing the polarization through 90° only there is a possibility for measuring unpolarized scattering cross sections. If a solenoid is used, the same goal is achieved by recording the scattered intensities when no field is applied, because in this case the reaction and scattering planes are at right angles to each other.

Finally, the pole pieces of the electromagnet may be designed so as to form integral parts of the neutron collimator assembly. The obvious advantage here is a concentration of the magnetic field within the collimator, implying efficient use of the magnet with negligible stray fields, and also optimum shielding of the detectors. An electromagnet has the disadvantage that the magnetic induction has to be measured separately, because it is not linearly related to the excitation current. Further, careful demagnetization has to be performed between successive runs.

3. Description of the precession magnet and its associated equipment

3.1 Mechanical part

The mechanical design of the precession magnet is apparent from the simplified cross sectional view given in fig. 3. The two excitation coils - electrically operated in parallel - are encased in a thick-walled soft-iron (Stg Perm [x]) box of outer dimensions 55 x 56 x 63 cm, effectively enclosing all magnetic field lines. The area of each of the two pole faces is 6 x 40 cm^2, and their mutual distance is equal to 4.5 cm. The effective air gap, however, is determined by the soft-iron side parts of the collimator, and the characteristic numbers for the present set-up are the following:

entrance air gap	16.6 mm
middle air gap	25.0 mm
exit air gap	44.4 mm

The two excitation coils [xx] are wound on copper forms, each divided into seven sections so that each section contains 170 turns of 1.6 x 2.5 mm copper wire. The number of turns for the whole magnet is 2380. The electrical insulation of the copper wire as well as the copper forms turned out to be a formidable obstacle to the faithful operation of the precession magnet. The final choice of wire became type DFH terephthalic acid polyester insulated copper wire [xxx] with an additional double-spun cotton insulation. A reliable electrical insulation of the copper forms was accomplished by spraying them with araldite doped with some quartz sand before winding. Further, melinex foils (thickness = 200 gauge) were placed between the copper wire and the walls of the copper forms. Also, melinex tape (thickness = 100 gauge) was interposed between the separate winding layers.

---

x Delivered by Domnarfvets Jernverk, Domnarvet, Sweden

xx Wound by Sandblom & Stohne, Stockholm, Sweden

xxx Delivered by Sieverts Kabelverk, Sundbyberg, Sweden

Each excitation coil is cooled by eight tubular cooling loops (inner diameter = 5 mm), and the total consumption of cooling water is 10 - 12 litres per minute. In order to prevent condensation of water vapor along the collimator the outlet temperature of the cooling water is kept constant slightly above room temperature. However, the field off-field on operation in the experimental routine implies a rather large variation in the heat production of the precession magnet. The cooling water is therefore preheated to a convenient thermostatically regulated temperature in a water boiler, and mixed with cold water before entering the precession magnet (see fig. 4). The mixing of preheated and cold water is governed by a temperature-sensitive probe in the outlet cooling water so that its temperature is kept constant within $\pm$ 0.5 ^{o}C.

3.2 Electronically stabilized power supply

The excitation coils of the precession magnet are powered by a 10 kW motor-generator [x] capable of delivering a maximum D.C. current of 45 A, corresponding to 53550 Ampere-turns. The D.C. output of this generator is controlled by a transistorized power supply. During normal operation the magnet current is maintained constant by means of negative feedback.

Fig. 5 shows a block diagram of the system. As indicated in fig. 5 the different units are located in different parts of the accelerator building. The electromagnet resides in the experimental hall, the motor-generator is in a machine room in the basement and the electronic equipment in the control room.

The electronic equipment consists of a power rectifier, an "auto" and a "power" amplifier, and a very-low frequency sine wave generator. The mains power to the control unit is taken through a safe-guard relay, ensuring that the cooling water to the electro-magnet is flowing before the circuits can be energized.

---

x Type RB 15/4 - ML10 delivered by AB Hägglund & Söner Örnsköldsvik, Sweden

The three-phase AC motor which drives the generator can be started by means of a push-button contactor located in the control room. The electronic unit supplies current to a main and an auxiliary field winding of the generator. The output current of the generator is proportional to the resultant Ampere-turns of these field windings. The maximum input to the main field winding is 5 A at 20 V, the generator output then being 45 A at 180 V. In the absence of control power a small residual current flows in the output circuit due the remanence field of the generator.

The control unit serves three purposes: 1) the magnetizing current is automatically stabilized to a predetermined value 2) the magnetizing current can be set manually to any desired value and 3) the electromagnet is demagnetized. Any one of these functions may be selected by pushing one of three control buttons labelled "Auto", "Man" and "Demagn" resp.

The normal mode of operation is obtained when the knob "Auto" is depressed for stabilizing the magnet current. In this case the current of the main stator winding is taken from the power rectifier and that of the auxiliary winding from the auto amplifier.

By means of a rheostat the current of the main winding is adjusted until a magnet current about 10 % lower than that desired is obtained. The auto amplifier senses the voltage drop across a 100 milliohm resistor in the magnet circuit and compares it with an adjustable reference voltage. The output of the auto amplifier is a current proportional to the difference between these two voltages. This output current is fed to the auxiliary stator winding thereby changing the generator output to a value which makes the input voltage difference nearly zero. The adjustable reference voltage is set to a value so as to give correct magnet current. Because of the feedback mechanism the current is stabilized to better than $\pm$ 0.5 %.

When the knob "Man" is depressed no current flows in the auxiliary winding. The current of the main winding is delivered by the power amplifier whose output is governed by a sine potentiometer. By turning the shaft of this potentiometer the output current of the amplifier can be continuously varied from + 5 to - 5 A. A corresponding variation is obtained in the main circuit and thus the magnet current can be manually set to any desired value.

In the "demagnetizing" mode the connections of the stator windings are the same as in the manual mode, but a decreasing voltage, generated by a "time constant" circuit, is applied at the sine potentiometer and simultaneously the shaft is slowly rotated (6 rpm) by a motor. The resulting effect is a damped sinusoidal output of the power amplifier and consequently a decreasing sinusoidal current through the precession magnet. When, after about 10 - 12 cycles, the voltage across the sine potentiometer has decreased to practically zero, a relay, short-circuiting the magnet coil, is actuated. The purpose of this relay is to remove the residual generator current from the magnet winding when - after the degaussing operation - the field has to be zero.

3.3 Auxiliary equipment

Readings of the excitation currents are taken by means of a Weston Model 1971 panel instrument (accuracy $\pm$ 0.5 %), whereas the magnetic induction is measured by means of a Rawson-Lush Type 820S rotating-coil Gauss-meter* having an accuracy of $\pm$ 0.1 %. The probe locations of the Gauss-meter can either be in the central part of the collimator, or peripherally where it does not interfere with the flight paths of the fast-neutrons.

4. Theory of operation

A general theory of the effect of a transverse magnetic field on the polarization of a fast-neutron beam and the associated effect on the left-right ratio is given in ref. [16], and will not be repeated here.

5. Performance

5.1 Magnetization curves

The magnetic properties of the precession magnet are displayed in fig. 6 where two magnetization curves are depicted, one obtained with the induction-sensitive probe located in the central part of the collimator, and the other with the probe in the peripheral position.

---

* Delivered by Rawson Electrical Instrument Co
110 Potter Street, Cambridge 42, Massachusetts, U.S.A.

As was to be expected these curves are constant fractions of each other, implying a justification of an important assumption made in ref. [16], namely that the magnetic field configuration is independent of field strength. In the following we therefore use the peripheral readings as convenient measures of the field intensities produced by the precession magnet.

Evidently both magnetization curves are linear for excitation currents up to approximately 20 Amperes, although no pronounced saturation takes place even at the maximum excitation current available. The remarkable properties of Stg Perm cast-iron for the present purpose become even more manifest when it is noted that for the demagnetized state a characteristic reading of the magnetic induction (probe in central position) is 6 Gauss.

5.2 Stray magnetic fields

As a convenient instrument for investigation of the existence of eventual stray fields a sensitive clip-on Ampere-meter (Hewlett-Packard Model 428A) with the clip opened was used. Although actually not calibrated in terms of magnetic induction it was rather easy to find a maximum reading caused by the magnetic field of the earth, and we therefore used this reading as a reference unit for stray magnetic induction.

An extensive search for stray fields was conducted both in the detector space and also at the position of the target spot. It turned out that in the whole detector space no measurable influence of stray fields was present. We are therefore safe to conclude that the detectors are not harmfully affected by the presence of the precession magnet. This is even more true when it is borne in mind that the detectors are equipped with special magnetic shields (see refs. [2 and 14a - 15b] for details). - At the position of the target spot some stray field influence was measurable, but even its maximum value was no more than about 10 times the effect of the field of the earth. - Further, an integral test of eventual harmful effects of stray magnetic fields on the target spot and the photo-multipliers was performed by observing the precession properties of the magnet at some field value, and then observing the same effect when the field direction was reversed. No difference between these experiments was observed (see refs. [2 and 14a - 15b]).

5.3 Precession properties

The precession properties of the magnet were investigated by using the set-up schematically depicted in fig. 3. Polarized fast-neutrons were obtained at 50^{o} (lab. syst.) from the $Li^7(p,n)Be^7$ reaction taking place in an oscillating target assembly closely resembling the original Argonne design. The collimated neutrons were scattered from a cylindrical natural carbon sample (dimensions: 40 mm ∅ x 80 mm), and finally detected at equal nominal scattering angles by means of two NE 102A plastic phosphors coupled to Philips AVP 56 photomultipliers by means of light pipes. Details of the associated quite elaborate electronic equipment are found in refs. [2, 15a, b and 17], and no account of them will be given here. The nominal scattering angle chosen, i.e. 42^{o} (lab. syst.), was largely determined by the expected maximum polarization at 45^{o} (c-of-m syst.) in $n + C^{12}$ elastic scattering in the MeV energy range [18].

The experimental routine was the following one: First, the precession magnet was left in a demagnetized state, and the scattering sample was brought to the "in" position by means of a pneumatic valve. Secondly, the number of counts in Detector 1 and Detector 2 (from now on referred to as Right Detector and Left Detector resp.) was recorded for some preset number of monitor counts. Further, the sample was brought to the "out" position, and a background run was made. The counting rate of scattered fast-neutrons in the left, resp. right detector is denoted C_o^L, resp. C_o^R, where the lower index refers to zero magnetic field. The ratio χ_o of these counting rates is consequently given by

$$\chi_o = \left(\frac{C_o^L}{C_o^R}\right) = \left(\frac{C^L}{C^R}\right)_o \qquad (2)$$

The precession magnet was now set at some convenient field value, and again the ratio

$$\chi_B = \left(\frac{C_B^L}{C_B^R}\right) = \left(\frac{C^L}{C^R}\right)_B \qquad (3)$$

of the counting rates of scattered neutrons was determined. We particularly point out that a separate background run was made when the magnet was in the magnetized state.

For the subsequent data treatment we chose to plot the ratio χ_o/χ_B as a function of the magnetic induction B^{x}. By means of a digital computer program [19] all data points were adjusted to the theoretical curve

$$\frac{\chi_o}{\chi_B} = \frac{1-(\overline{P_1P_2})}{1+(\overline{P_1P_2})}\;\frac{1+(\overline{P_1P_2})\cos\left(\frac{B}{B_\pi}\pi\right)}{1-(\overline{P_1P_2})\cos\left(\frac{B}{B_\pi}\pi\right)} \tag{4}$$

where $(\overline{P_1P_2})$ is a suitably defined average polarization product over the finite geometry in question (see ref. [16]). Typical precession curves are displayed in figs. 7-9, where in particular the necessary magnetic inductions B_π for precessing the incident polarizations $\vec{P}_1$ through 180^o are quoted. Further the whole body of precession data available is presented in Table 1.

E_p MeV	E_n MeV	B_π kGauss
2.987	1.062 $\pm$ 0.027	?
3.261	1.317 $\pm$ 0.024	3.737 $\pm$ 0.214
3.613	1.639 $\pm$ 0.021	4.960 $\pm$ 0.162
3.712	1.736 $\pm$ 0.017	4.291 $\pm$ 0.332
3.793	1.807 $\pm$ 0.020	4.651 $\pm$ 0.194
3.880	1.890 $\pm$ 0.016	5.528 $\pm$ 0.242
3.984	1.983 $\pm$ 0.016	5.085 $\pm$ 0.165
4.049	2.041 $\pm$ 0.018	4.997 $\pm$ 0.184
4.298	2.266 $\pm$ 0.019	5.773 $\pm$ 0.144
4.395	2.355 $\pm$ 0.018	5.819 $\pm$ 0.081
4.498	2.450 $\pm$ 0.017	5.756 $\pm$ 0.149

Table 1.

Summary of available precession data.

---

^{x} Note that no correction for multiple scattering has been applied, because it does not significantly change the location of the maximum of χ_o/χ_B.

We observe that even for the highest neutron energy the maximum field strength is sufficient for precessing the polarization through more than 360°. This is a most convenient feature of the present magnet, because the quality of the fits is highly influenced by the possibility of data-taking symmetrically around B_{π}. Observe further that the neutron energy uncertainties quoted only take care of finite target thickness effects, but do not include the energy broadening caused by finite geometry.

As has been proved in ref. [16] the dependence of B_{π} on $\bar{\bar{E}}_n$ is described by

$$B_{\pi} \approx \pi \sqrt{2}\, \frac{\hbar \cdot s}{\mu \cdot \mu_N}\, \frac{1}{L_{eff}}\, \frac{1}{\sqrt{m}} \sqrt{\bar{\bar{E}}_n} = k \sqrt{\bar{\bar{E}}_n} \qquad (5)$$

where L_{eff} is the effective length of the precession field.

Using the principle of least squares we adjusted our data to a straight line in the $\sqrt{\bar{\bar{E}}_n}$-B_{π}-plane, and found the relation

$$B_{\pi} = (3.718 \pm 0.033)\, \sqrt{\bar{\bar{E}}_n}\ \text{kGauss} \quad (\bar{\bar{E}}_n \text{ in MeV}) \qquad (6)$$

Correcting for the lower reading of the magnetic induction at the peripheral position of the Gauss-meter we obtain

$$B_{\pi}^{c} = \frac{1090}{621}\, (3.718 \pm 0.033)\, \sqrt{\bar{\bar{E}}_n}\ \text{kGauss} \qquad (7)$$

$$= (6.525 \pm 0.058)\, \sqrt{\bar{\bar{E}}_n}\ \text{kGauss}$$

and further

$$L_{eff}^{c} = (36.3 \pm 0.4)\ \text{cm} \qquad (8)$$

Comparison with the theoretical expression $B_{\pi}^{c} = 5.930\ \sqrt{\bar{\bar{E}}}$ kGauss yields the conclusion that the average induction is lower than the central induction in the ratio $5.930 : 6.525 = 0.91 < 1$, which was to be expected when due consideration is taken to the special design of the collimator. Also, the design requirements are very well fulfilled, because the present magnet can precess through 180° the polarization of neutrons of maximum energy = $\left(\frac{12.6}{3.718}\right)^2$ MeV = ≈ 11.5 MeV.

A more exact determination of L_{eff} can be performed by taking due consideration to the finite-geometry effects in the experiment. These effects, however, present numerical difficulties which require digital computer techniques for their sucessful solution. A Monte Carlo program [20] simulating the experimental conditions is presently under preparation, and may in particular be used for a determination of L_{eff} from the condition $\frac{\partial}{\partial L_{eff}}(\chi_o/\chi_{B_\pi}) = 0$.

Finally, one remark will be made about possible harmful effects of the inhomogeneities of the magnetic field. As has been proved in Appendix II of ref. [21] no lateral displacement of the collimated fast-neutron beam is likely to take place, implying the same first-scattering densities as when no magnetic field is applied at all. Also, any quantum effects on the polarized fast-neutron beam are extremely unlikely in virtue of the short transit times involved. For all practical purposes therefore the present precession magnet behaves as if it produced an ideal homogeneous field.

6. Summary

In this paper we have given a general discussion of the advantages in using transverse magnetic fields in fast-neutron polarization experiments. Design details are presented for a powerful electromagnet capable of precessing through 180^o the polarization of fast-neutrons of maximum energy = 11.5 MeV. The characteristics of performance are displayed in the form of typical precession curves from which B_π has been obtained, and finally summarized in Table 1. Also, a separate determination of B_π as a function of energy has been performed. Finally, the superior qualities of the present precession magnet are manifest through negligible stray magnetic fields at the locations of the target spot and the photomultipliers.

7. Acknowledgements

The authors wish to express their gratitude to Sieverts Kabelverk and to Sandblom & Stohne for excellent work. Our thanks are further due to U. Wetzenstein for his araldite insulation recipe, to the central workshop, AB Atomenergi for splendid solutions to many complicated technical problems, and also to L. Aringe for his mechanical skill and benevolent help in data-taking. Finally, we want to thank Dr. R. Pauli for his constant interest in the design and the operation of the precession magnet.

References

1. HAEBERLI, W,
Polarization of Neutrons in Reactions and Scattering.
Fast Neutron Physics, Ed. J.B. Marion and J.L. Fowler,
Part 2: Experiments and Theory, Interscience Publ.,
Inc., New York, 1963 p. 1379-1427.

2. ASPELUND, O and TRUMPY, G, to be published.

3a. WILSON, R, private communication to HILLMAN, P,
STAFFORD, G H and WHITEHEAD, C (see 3b).

3b. HILLMAN, P, STAFFORD, G H and WHITEHEAD, C,
A New Method of Measuring Asymmetries in Neutron Polarization Experiments,
Nuovo Cim., Ser. X, 4 (1956) 67-74.

4. DUBBELDAM, P S, JONKER, C C and HEEMSKERK, F J,
Measurement of the Polarization of D-D-neutrons by a
Solenoid.
Nucl. Instr. & Meth. 4 (1959) 234-238.

5. DUBBELDAM, P S and WALTER, R L,
Polarization of D-D-neutrons for Deuteron Energies from
1.9 to 11 MeV.
Nucl. Phys. 28 (1961) 414-425.

6. WONG, C et al.,
Polarization of 24-MeV Neutrons Elastically Scattered from
C, Al, Fe, Sn, Pb and Bi.
Phys. Rev. 128 (1962) 2339-2344.

7. PERKINS, R B and SIMMONS, J E,
Polarization in Neutron-Proton Scattering at 23.1 MeV.
Phys. Rev. 130 (1963) 272-275.

8. GLEYVOD, R et al.,
Messung des Polarisationsvermögens von Sauerstoff für d, d-Neutronen von 2,5 bis 3,2 MeV Energie.
Helv. Phys. Acta 36 (1963) 287-297.

9. TRUMPY, G,
AB Atomenergi, Internal Report TPM-RFX-60-1 (1960).

10. DARDEN, S E, KELSEY, C A and DONOGHUE, T R,
Polarization of Neutrons Scattered from Li^6 and Li^7.
Helv. Phys. Acta Suppl. 6 (1961) 269-276.

11. FERGUSON, A T G and WHITE, R E,
Polarization in Neutron-Deuteron Elastic Scattering below
1.0 MeV. Nucl. Phys. 33 (1962) 477-481.

12. ELWYN, A J, LANE, R O and LANGSDORF Jr, A,
Polarization and Differential Cross Sections in n-d Scattering.
Phys. Rev. 128 (1962) 779-789.

13. BEGHIAN, L E et al.,
Neutron Polarization in the MeV Region by Elastic Scattering on C, O and D.
Nucl. Phys. 42 (1963) 1-20.

14a. ASPELUND, O and TRUMPY, G,
Fast Neutron Polarization Flip by a Transverse Magnetic Field.
AB Atomenergi, Internal Report RFX-72 (1961).

14b. ASPELUND, O, and TRUMPY, G, talk given at the Biannual Meeting of the Swedish Physical Society, Lund, 2-4 June 1961.

14c. ASPELUND, O and TRUMPY, G,
Fast Neutron Polarization Flip by a Transverse Magnetic Field.
Arkiv Fysik 22 (1962) 391.

15a. ASPELUND, O,
An Apparatus for Investigation of Neutron Polarization in the MeV Region.
AB Atomenergi, Internal Report RFX-97 (1962).

15b. ASPELUND, O, talk given at the Annual Meeting of the Norwegian Physical Society, Kjeller and Oslo, 21-23 May 1962.

16. ASPELUND, O,
A General Formalism for Numerical Evaluation of the Polarization of Fast-Neutron by Means of Finite-Geometry Measurements of the Left-Right Ratio.
AB Atomenergi, Internal Report FFN-5 (1964).

17. ASPELUND, O,
A Fast Time-to-Pulse Height Converter.
AE-97 (1962) and Nucl. Instr. & Meth. 23 (1963) 1-9.

18. WILLS Jr, J E et al.,
Scattering of Fast Neutrons from C^{12} and F^{19}.
Phys. Rev. 109 (1958) 891-897.

19. NÄSLUND, G, private communication.

20. ASPELUND, O and GUSTAFSSON, B, to be published.

21. ASPELUND, O, BJÖRKMAN, J and TRUMPY, G,
An Electromagnet for Precession of the Polarization of Fast-Neutrons.
AB Atomenergi, Internal Report FFN-11 (1965).

Appendix

A. Required magnetic induction for precessing the fast-neutron polarization through 180°

The Larmor frequency ω_L is given by the expression

$$\omega_L = \frac{\mu_n \cdot B}{\hbar \cdot s} = \frac{\mu \cdot \mu_N}{\hbar \cdot s} B \qquad (9)$$

where

$\mu_n = \mu \cdot \mu_N$ = magnetic moment of the neutron

μ = magnetic moment of the neutron in units of the nuclear magneton

μ_N = nuclear magneton

s = intrinsic angular momentum = spin } of the neutron

$\hbar$ = Planck's constant divided by 2π

Numerical values

$\mu = -1.913148 \pm 0.000066$ nuclear magnetons

$\mu_N = (5.0505 \pm 0.0004)\, 10^{-27}$ Joule/Tesla

$s = \frac{1}{2}$

$\hbar = (1.0545 \pm 0.00007)\, 10^{-34}$ Joule sec

The necessary magnetic induction B_π for precessing the polarization $\vec{P}_1$ through π radians is given by the condition

$$\omega_L \cdot t_L = \pi \qquad (10)$$

where $t_L = \frac{72.3}{\sqrt{E_n}} L$ nsec is the neutron flight time over the distance L. Assuming that the field is effective only between the pole pieces B_π is found to be

$$B_\pi = 5.930 \sqrt{\overline{E}_n} \text{ kGauss} \quad (\overline{E}_n \text{ in MeV}) \quad . \tag{11}$$

which for neutrons of energy $\overline{E}_n = 10$ MeV yields $B_\pi = 18.75$ kGauss. Here no consideration has been taken to any inhomogeneity of the field.

B. Required accuracy of B_π

Obviously the component $P_1^\perp$ of the neutron polarization normal to the direction of flight is given by

$$P_1^\perp = P_1 \; |\cos(\omega_L t_L)| \tag{12}$$

Suppose further that B_π is known within $\pm \Delta B$. We then have

$$P_1^{\perp\prime} = P_1 \; |\cos(\pi \pm 1.83 \times 10^4 \;\; \Delta B \frac{72.3}{\sqrt{\overline{E}_n}} \; 0.4 \times 10^{-9})\;| \tag{13}$$

$$= P_1 \cos(\Delta\alpha)$$

where

$$\Delta\alpha = 5.3 \times 10^{-4} \frac{\Delta B}{\sqrt{\overline{E}_n}} \tag{14}$$

The relative uncertainty in our knowledge of the normal component is given by

$$\frac{P_1 - P_1^{\perp\prime}}{P_1} = 1 - \cos(\Delta\alpha) = \frac{(\Delta\alpha)^2}{2} - 0\,(\;(\Delta\alpha)^4\;) \tag{15}$$

Requiring that this uncertainty shall be less than 1 % yields the following condition

$$\frac{(\Delta\alpha)^2}{2} = \frac{1}{2}(5.3 \times 10^{-4} \;\; \frac{\Delta B}{\sqrt{\overline{E}_n}})^2 \leq \frac{1}{100} \tag{16}$$

Thus

$$\Delta B \leq \sqrt{\overline{E}_n} \;\; 264 \text{ Gauss} \tag{17}$$

Or

$$\frac{\Delta B}{B_{\pi}} \leq 5 \% \tag{18}$$

In other words, the requirements of accuracy in our knowledge of B_{π} are not very stringent.

C. Required accuracy of $B_{\pi/2}$

A similar calculation as the one outlined above yields for the relative normal component.

$$\frac{P_1^{\perp ''}}{P_1} = \sin \left(5.3 \times 10^{-4} \frac{\Delta B}{\sqrt{\overline{E}_n}}\right) \tag{19}$$

So, if we want this uncertainty to be less than 1 %, we have to terms of the third order

$$5.3 \times 10^{-4} \frac{\Delta B}{\sqrt{\overline{E}_n}} \leq \frac{1}{100} \tag{20}$$

Consequently

$$\Delta B \leq 19 \sqrt{\overline{E}_n'} \tag{21}$$

The required relative accuracy in $B_{\pi/2}$ is thus given by

$$\frac{\Delta B}{B_{\pi/2}} \leq 6 \ {}^{o}/oo \tag{22}$$

This is a very stringent requirement, but is nevertheless met by the servostabilized power supply feeding the field windings of the motor-generator.

Figure captions

1. Principle of the fast-neutron polarization experiment

Legend:

$\vec{k}$ = unit laboratory wave vector of incident charged-particle beam

$\vec{k}_n$ = unit laboratory wave vector of emitted fast-neutron beam

$\vec{k}_{n'}$ = unit laboratory wave vector of scattered fast-neutron beam

$\vec{n}_1 = \frac{[\vec{k} \times \vec{k}_n]}{|[\vec{k} \times \vec{k}_n]|}$ = unit normal vector to the reaction plane

$\vec{n}_2 = \frac{[\vec{k}_n \times \vec{k}_{n'}]}{|[\vec{k}_n \times \vec{k}_{n'}]|}$ = unit normal vector to the scattering plane

$\vec{P}_1(\theta_1) = P_1(\theta_1)\, \vec{n}_1$ = polarization of emitted fast-neutron beam

$\vec{P}_2(\theta_2) = P_2(\theta_2)\, \vec{n}_2$ = polarization of scattered fast-neutron beam

θ_1 = nominal reaction angle

θ_2 = nominal scattering angle

2. Larmor precession of the fast-neutron polarization by a transverse magnetic field.

3. Simplified cross sectional view of the mechnical set-up for the fast-neutron polarization experiment.

4. Schematic diagram of the cooling water system.

5. Block diagram of the electronically stabilized current supply.

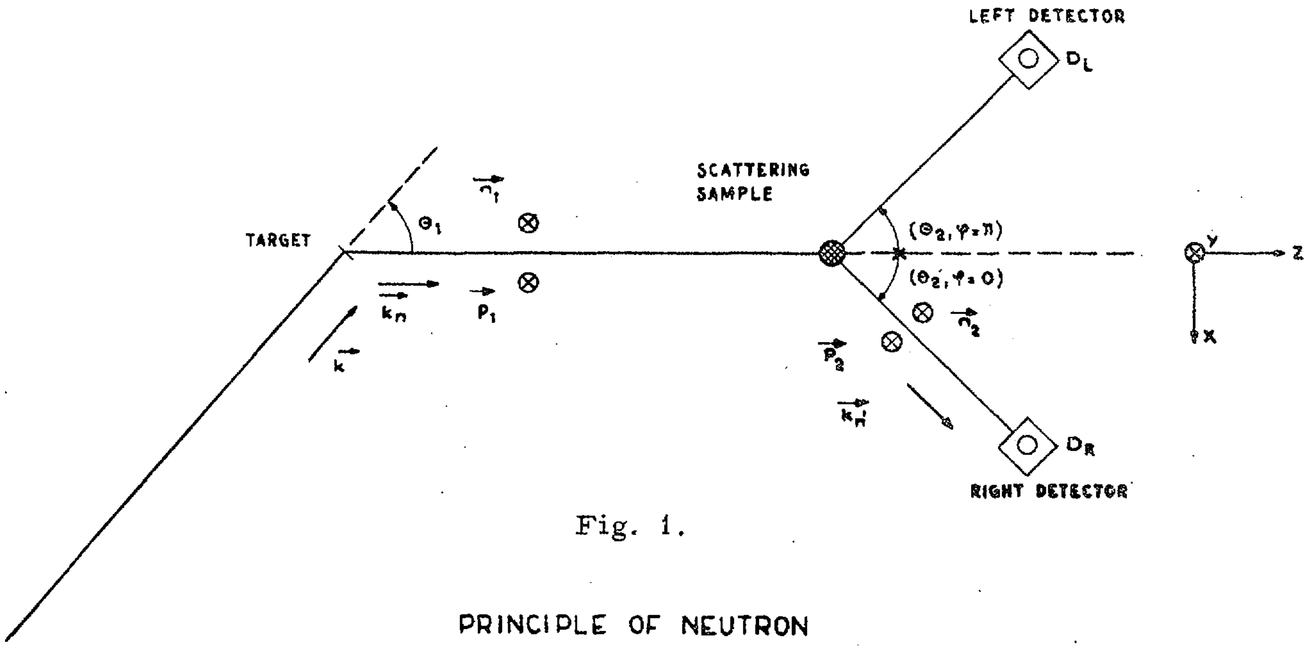

Fig. 1.

PRINCIPLE OF NEUTRON
POLARIZATION EXPERIMENT

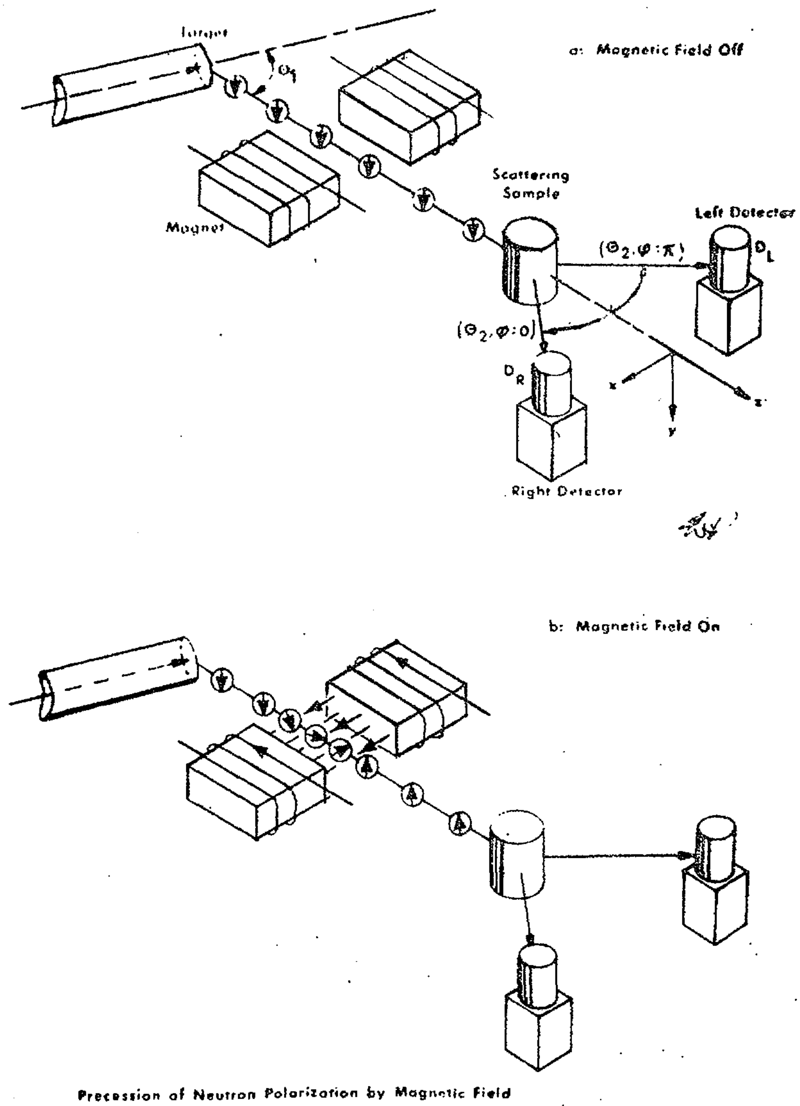

Fig. 2.

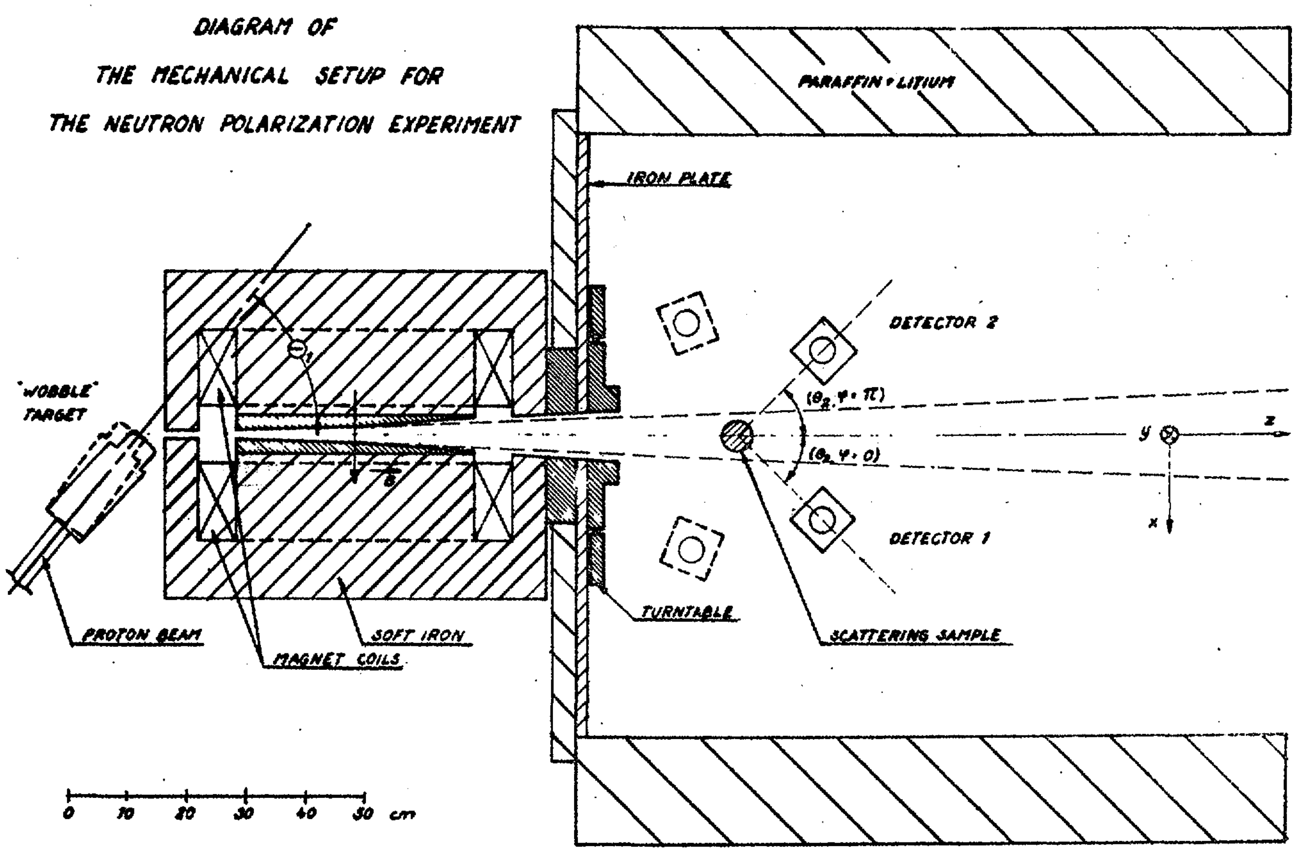
DIAGRAM OF
THE MECHANICAL SETUP FOR
THE NEUTRON POLARIZATION EXPERIMENT
PARAFFIN + LITIUM
IRON PLATE
DETECTOR 2
DETECTOR 1
"WOBBLE" TARGET
PROTON BEAM
MAGNET COILS
SOFT IRON
TURNTABLE
SCATTERING SAMPLE
0 10 20 30 40 50 cm

Fig. 3.

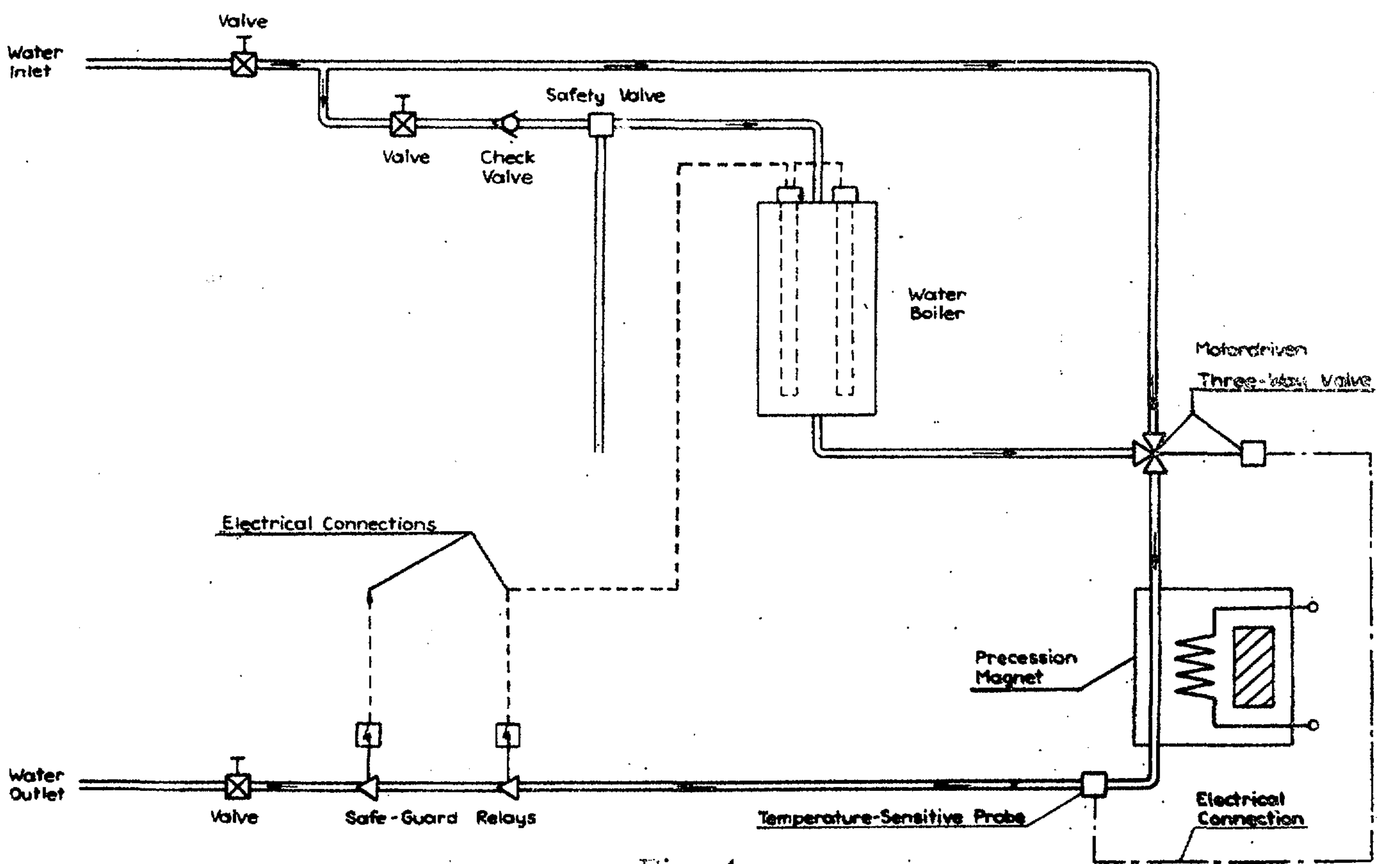
Water Inlet
Valve
Valve
Check Valve
Safety Valve
Water Boiler
Motordriven
Three-Way Valve
Electrical Connections
Precession Magnet
Water Outlet
Valve
Safe-Guard
Relays
Temperature-Sensitive Probe
Electrical Connection

Fig. 4.

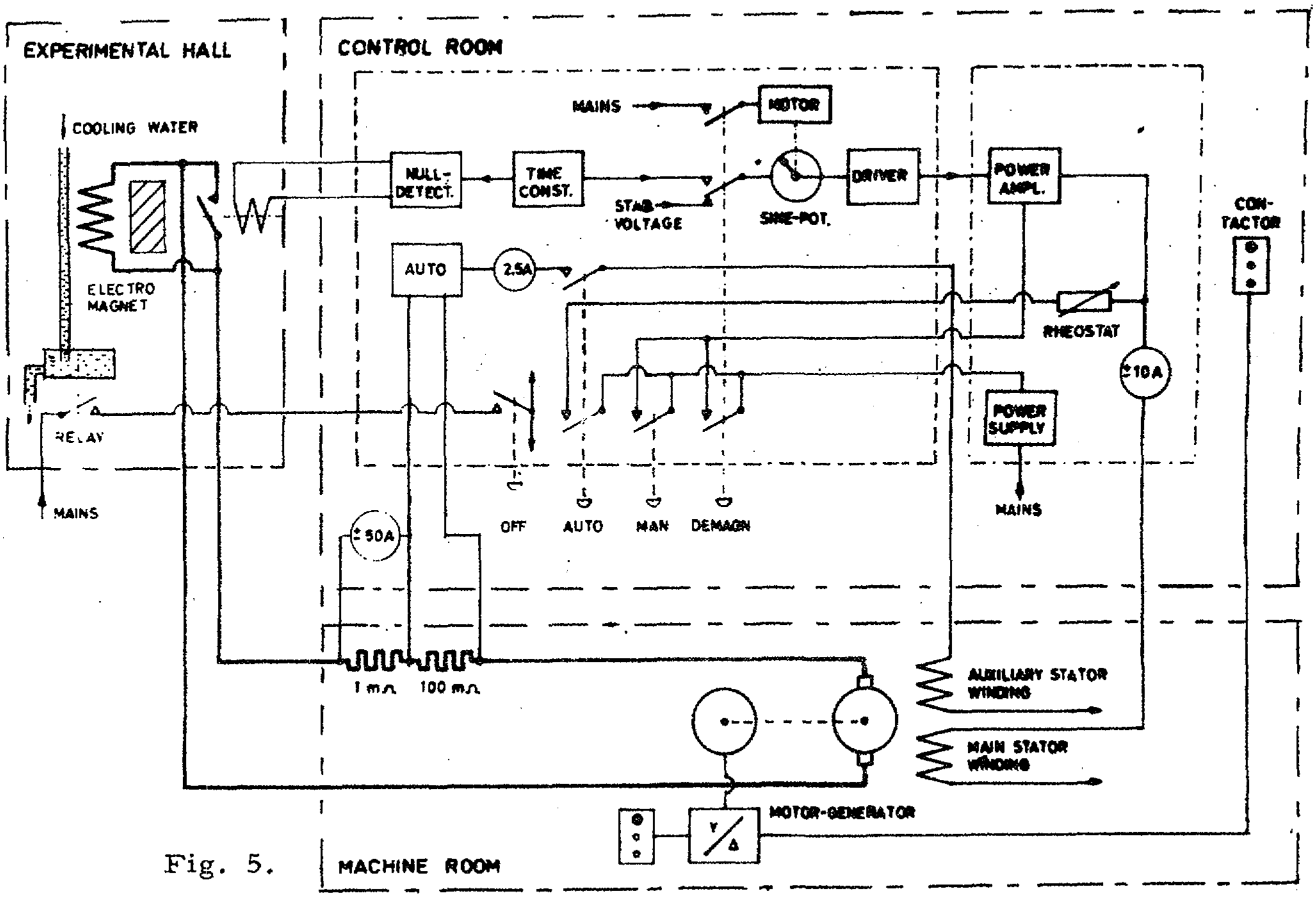

Fig. 5.

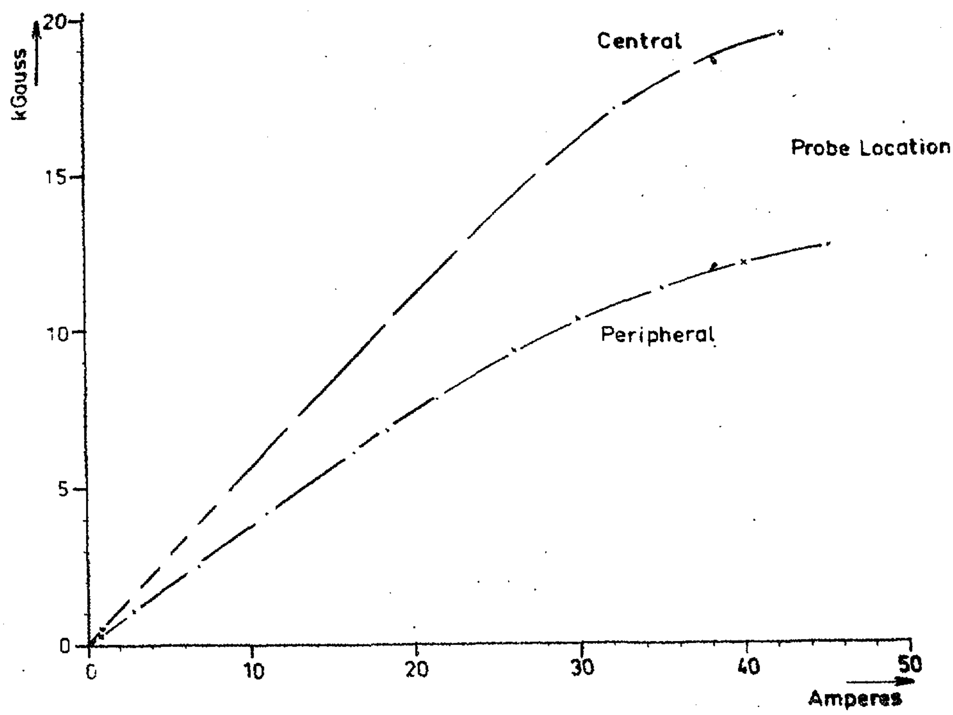

Magnetization Curves of the Precession Magnet.

Fig. 6.

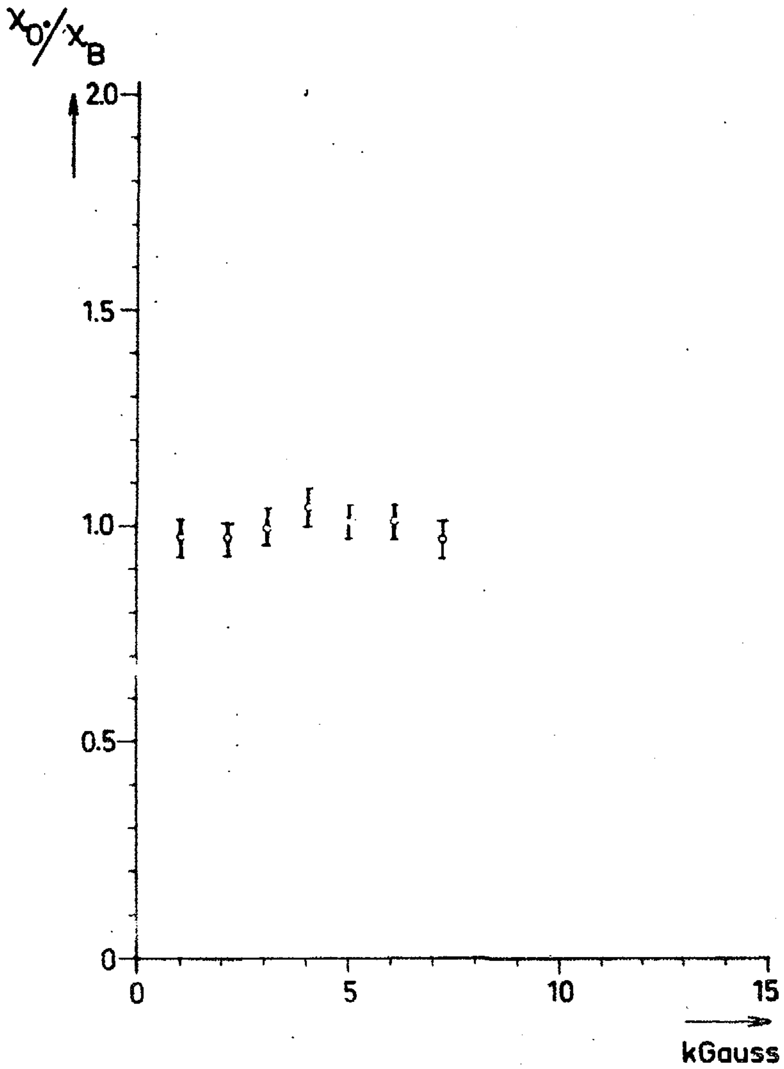

Fig. 7. Precession Curve No.1

E_p = 2.987 MeV; E_n = 1.062±0.027 MeV

Θ_1 = 50° ; Θ_2 = 42°

B_π = ?

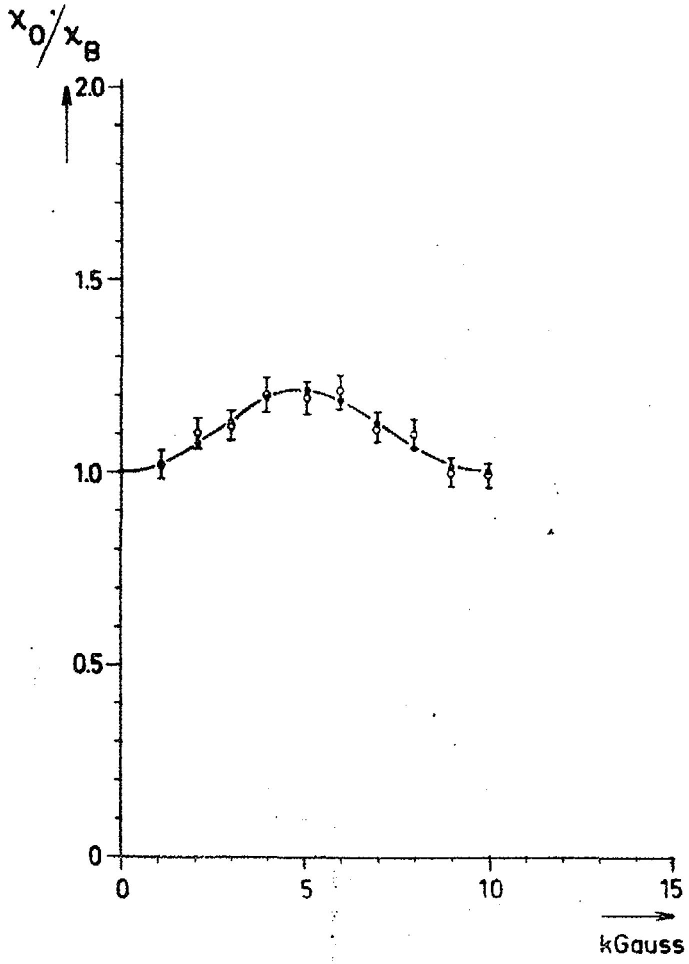

Fig. 8. Precession Curve No. 3

E_p = 3.613 MeV; E_n = 1.639 ± 0.021 MeV

Θ_1 = 50° ; Θ_2 = 42°

B_π = 4.960 + 0.162 kGauss

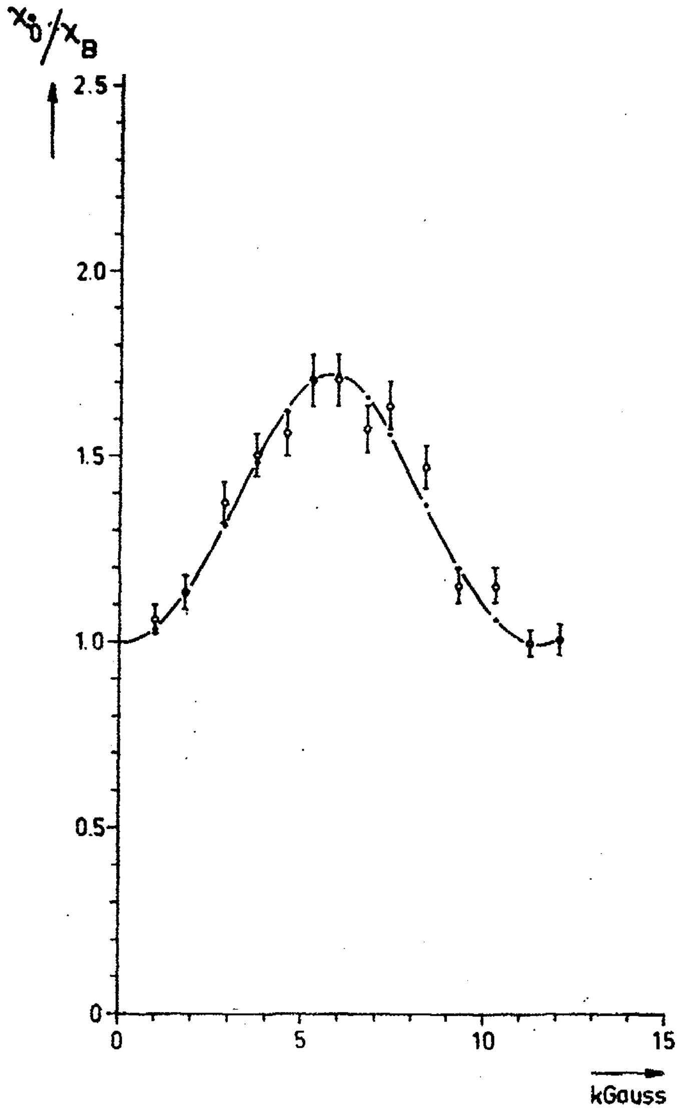

Fig. 9. Precession Curve No.11

$E_p = 4.498$ MeV; $E_n = 2.450 \pm 0.017$ MeV

$\Theta_1 = 50^\circ$; $\Theta_2 = 42^\circ$

$B_\pi = 5.756 \pm 0.149$ kGauss

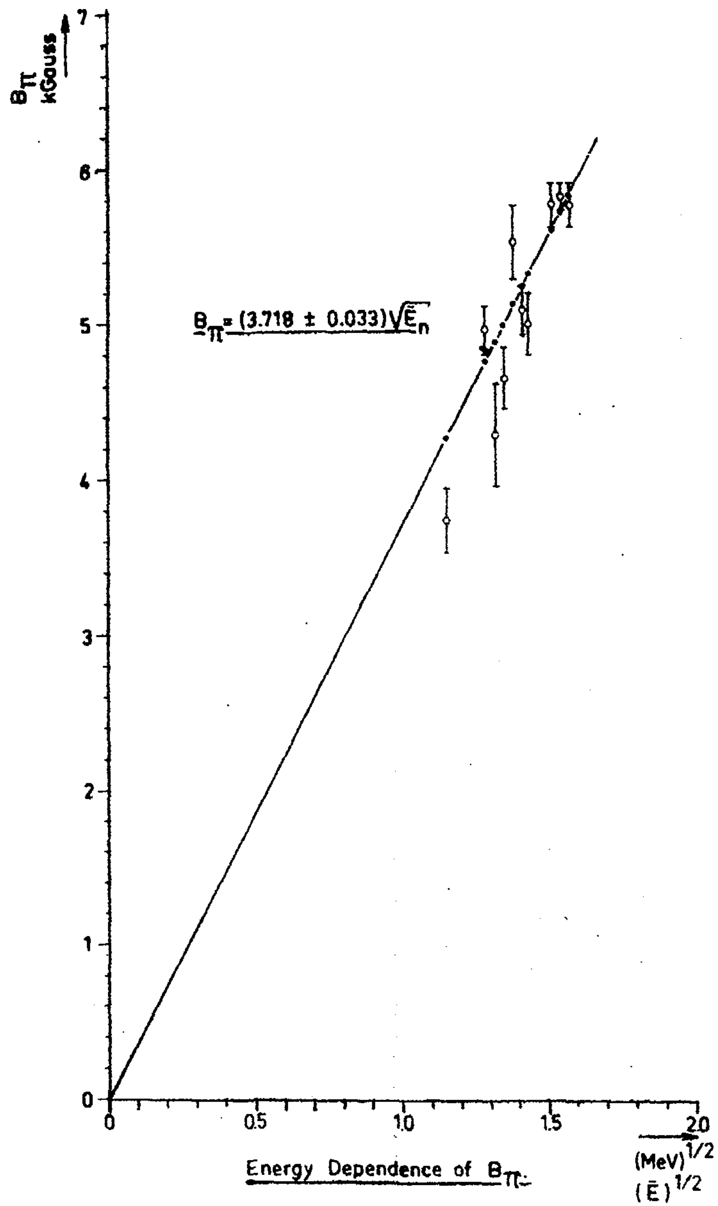

Fig. 10.

LIST OF PUBLISHED AE-REPORTS

1—110. (See the back cover earlier reports.)

111. The paramagnetism of small amounts of Mn dissolved in Cu-Al and Cu-Ge alloys. By H. P. Myers and R. Westin. 1963. 7 p. Sw. cr. 8:—.
112. *Determination of the absolute disintegration rate of Cs^{137}-sources by the tracer method.* By S. Hellström and D. Brune. 1963. 17 p. Sw. cr. 8:—.
113. An analysis of burnout conditions for flow of boiling water in vertical round ducts. By K. M. Becker and P. Persson. 1963. 28 p. Sw. cr. 8:—.
114. Measurements of burnout conditions for flow of boiling water in vertical round ducts (Part 2). By K. M. Becker, et al. 1963. 29 p. Sw. cr. 8:—.
115. Cross section measurements of the $^{58}Ni(n, p)^{58}Co$ and $^{29}Si(n, _m)^{26}Mg$ reactions in the energy range 2.2 to 3.8 MeV. By J. Konijn and A. Lauber 1963. 30 p. Sw. cr. 8:—.
116. Calculations of total and differential solid angles for a proton recoil solid state detector. By J. Konijn, A. Lauber and B. Tollander. 1963. 31 p. Sw. cr. 8:—.
117. Neutron cross sections for aluminium. By L. Forsberg. 1963. 32 p. Sw. cr. 8:—.
118. Measurements of small exposures of gamma radiation with $CaSO_4$:Mn radiothermoluminescence. By B. Bjärngard. 1963. 18 p. Sw. cr. 8:—.
119. Measurement of gamma radioactivity in a group of control subjects from the Stockholm area during 1959—1963. By I. Ö. Andersson, I. Nilsson and Eckerstig. 1963. 19 p. Sw. cr. 8:—.
120. The *thermox* process. By O. Tjälldin. 1963. 38 p. Sw. cr. 8:—
121. The transistor as low level switch. By A. Lydén. 1963. 47 p. Sw. cr. 8:—.
122. The planning of a small pilot plant for development work on aqueous reprocessing of nuclear fuels. By T. U. Sjöborg, E. Haeffner and Hultgren. 1963. 20 p. Sw. cr. 8:—.
123. The neutron spectrum in a uranium tube. By E. Johansson, E. Jonsson, M. Lindberg and J. Mednis. 1963. 36 p. Sw. cr. 8:—.
124. Simultaneous determination of 30 trace elements in cancerous and non-cancerous human tissue samples with gamma-ray spectrometry. K. Samsahl, D. Brune and P. O. Wester. 1963. 23 p. Sw. cr. 8:—.
125. Measurement of the slowing-down and thermalization time of neutrons in water. By E. Möller and N. G. Sjöstrand. 1963. 42 p. Sw. cr. 8:—.
126. Report on the personell dosimetry at AB Atomenergi during 1962. By K.-A. Edvardsson and S. Hagsgård. 1963. 12 p. Sw. cr. 8:—.
127. A gas target with a tritium gas handling system. By B. Holmqvist and T. Wiedling. 1963. 12 p. Sw. cr. 8:—.
128. Optimization in activation analysis by means of epithermal neutrons. Determination of molybdenum in steel. By D. Brune and K. Jirlow. 1963. 11 p. Sw. cr. 8:—.
129. The P_1-approximation for the distribution of neutrons from a pulsed source in hydrogen. By A. Claesson. 1963. 18 p. Sw. cr. 8:—.
130. Dislocation arrangemants in deformed and neutron irradiated zirconium and zircaloy-2. By R. B. Roy. 1963. 18 p. Sw. cr. 8:—.
131. Measurements of hydrodynamic instabilities, flow oscillations and burnout in a natural cirkulation loop. By K. M. Becker, R. P. Mathisen, O. Eklind and B. Norman. 1964. 21 p. Sw. cr. 8:—.
132. A neutron rem counter. By I. Ö. Andersson and J. Braun. 1964. 14 p. Sw. cr. 8:—.
133. Studies of water by scattering of slow neutrons. By K. Sköld, E. Pilcher and K. E. Larsson. 1964. 17 p. Sw. cr. 8:—.
134. The amounts of As, Au, Br, Cu, Fe, Mo, Se, and Zn in normal and uraemic human whole blood. A comparison by means neutron activation analysis. By D. Brune, K. Samsahl and P. O. Wester. 1964. 10 p. Sw. cr. 8:—.
135. A Monte Carlo method för the analysis of gamma radiation transport from distributed sources in laminated shields. By M. Leimdörfer. 1964. 28 p. Sw. cr. 8:—.
136. Ejection of uranium atoms from UO_2 by fission fragments. By G. Nilsson. 1964. 38 p. Sw. cr. 8:—.
137. Personell neutron monitoring at AB Atomenergi. By S. Hagsgård and C.-O. Widell. 1964. 11 p. Sw. cr. 8:—.
138. Radiation induced precipitation in iron. By B. Solly. 1964. 8 p. Sw. cr. 8:—.
139. Angular distributions of neutrons from (p, n)-reactions in some mirror nuclei. By L. G. Strömberg, T. Wiedling and B. Halmqvist. 1964. 28 p. Sw. cr. 8:—.
140. An extended Greuling-Goertzel approximation with a P_n -approximation in the angular dependence. By R. Håkansson. 1964. 21 p. Sw. cr. 8:—.
141. Heat transfer and pressure drop with rough surfaces, a literature survey. By A. Bhattachayya. 1964. 78 p. Sw. cr. 8:—.
142. Radiolysis of aqueous benzene solutions. By H. Christensen. 1964. 50 p. Sw. cr. 8:—.
143. Cross section measurements for some elements suited as thermal spectrum indicators: Cd, Sm, Gd and Lu. By E. Sokolowski, H. Pekarek and E. Jonsson. 1964. 27 p. Sw. cr. 8:—.
144. A direction sensitive fast neutron monitor. By B. Antolkovic, B. Holmqvist and T. Wiedling. 1964. 14 p. Sw. cr. 8:—.
145. A user's manual for the NRN shield design method. By L. Hjärne. 1964. 107 p. Sw. cr. 10:—.
146. Concentration of 24 trace elements in human heart tissue determined by neutron activation analysis. By P. O. Wester. 1964. 33 p. Sw. cr. 8:—.
147. Report on the personnel Dosimetry at AB Atomenergi during 1963. By K.-A. Edvardsson and S. Hagsgård. 1964. 16 p. Sw. cr. 8:—.
148. A calculation of the angular moments of the kernel for a monatomic gas scatterer. By R. Håkansson. 1964. 16 p. Sw. cr. 8:—.
149. An anion-exchange method for the separation of P-32 activity in neu*tron-irradited biological material.* By K. *Samsahl.* 1964. 10 p. Sw. cr. 8:—.
150. Inelastic neutron scattering cross sections of Cu^{63} and Cu^{65} in the energy region 0.7 to 1.4 MeV. By B. Holmqvist and T. Wiedling. 1964. 30 p. Sw. cr. 8:—.
151. Determination of magnesium in needle biopsy samples of muscle tissue by means of neutron activation analysis. By D. Brune and H. E. Sjöberg. 1964. 8 p. Sw. cr. 8:—.
152. Absolute El transition probabilities in the dofermed nuclei Yb^{177} and Hf^{179}. By Sven G. Malmskog. 1964. 21 p. Sw. cr. 8:—.
153. *Measurements of burnout conditions for flow of boiling water in vertical* 3-rod and 7-rod clusters. By K. M. Becker, G. Hernborg and J. E. Flinta. 1964. 54 p. Sw. cr. 8:—.
154. Integral parameters of the thermal neutron scattering law. By S. N. Purohit. 1964. 48 p. Sw. cr. 8:—.
155. Tests of neutron spectrum calculations with the help of foil measurments in a D_2O and in an H_2O-moderated reactor and in reactor shields of concrete and iron. By R. Nilsson and E. Aalto. 1964. 23 p. Sw. cr. 8:—.
156. Hydrodynamic instability and dynamic burnout in natural circulation two-phase flow. An experimental and theoretical study. By K. M. Becker, S. Jahnberg, I. Haga, P. T. Hansson and R. P. Mathisen. 1964. 41 p. Sw. cr. 8:—.
157. Measurements of neutron and gamma attenuation in massive laminated shields of concrete and a study of the accuracy of some methods of calculation. By E. Aalto and R. Nilsson. 1964. 110 p. Sw. cr. 10:—.
158. A study of the angular distributions of neutrons from the Be^9 (p,n) B^9 *reaction at low proton energies.* By. B. Antolkovic', B. Holmqvist and T. Wiedling. 1964. 19 p. Sw. cr. 8:—.
159. A simple apparatus for fast ion exchange separations. By K. Samsahl. 1964. 15 p. Sw. cr. 8:—.
160. Measurements of the Fe^{54} (n, p) Mn^{54} reaction cross section in the neutron energy range 2.3—3.8 MeV. By A. Lauber and S. Malmskog. 1964. 13 p. Sw. cr. 8:—.
161. Comparisons of measured and calculated neutron fluxes in laminated iron and heavy water. By. E. Aalto. 1964. 15. p. Sw. cr. 8:—.
162. A needle-type p-i-n junction semiconductor detector for in-vivo measure*ment of beta tracer activity.* By A. Lauber and B. *Rosencrantz.* 1964. 12 p. Sw. cr. 8:—.
163. Flame spectro photometric determination of strontium in water and biological material. By G. Jönsson. 1964. 12 p. Sw. cr. 8:—.
164. The solution of a velocity-dependent slowing-down problem using case's eigenfunction expansion. By A. Claesson. 1964. 16 p. Sw. cr. 8:—.
165. Measurements of the effects of spacers on the burnout conditions for flow of boiling water in a vertical annulus and a vertical 7-rod cluster. By K. M. Becker and G. Hernberg. 1964. 15 p. Sw. cr. 8:—.
166. The transmission of thermal and fast neutrons in air filled annular ducts through slabs of iron and heavy water. By J. Nilsson and R. Sandlin. 1964. 33 p. Sw. cr. 8:—.
167. The radio-thermoluminescense of $CaSO_4$: Sm and its use in dosimetry. By B. Bjärngard. 1964. 31 p. Sw. cr. 8:—.
168. A fast radiochemical method for the determination of some essential trace elements in biology and medicine. By K. Samsahl. 1964. 12 p. Sw. cr. 8:—.
169. Concentration of 17 elements in subcellular fractions of beef heart tissue determined by neutron activation analysis. By P. O. Wester. 1964. 29 p. Sw. cr. 8:—.
170. Formation of nitrogen-13, fluorine-17, and fluorine-18 in reactor-irradiated H_2O and D_2O and applications to activation analysis and fast neutron flux monitoring. By L. Hammar and S. Forsén. 1964. 25 p. Sw. cr. 8:—.
171. Measurements on background and fall-out radioactivity in samples from the Baltic bay of Tvären, 1957—1963. By P. O. Agnedal. 1965. 48 p. Sw. cr. 8:—.
172. Recoil reactions in neutron-activation analysis. By D. Brune. 1965. 24 p. Sw. cr. 8:—.
173. A parametric study of a constant-Mach-number MHD generator with nuclear ionization. By J. Braun. 1965. 23 p. Sw. cr. 8:—.
174. Improvements in applied gamma-ray spectrometry with germanium semiconductor dector. By D. Brune, J. Dubois and S. Hellström. 1965. 17 p. Sw. cr. 8:—.
175. Analysis of linear MHD power generators. By E. A. Witalis. 1965. 37 p. Sw. cr. 8:—.
176. Effect of buoyancy on forced convection heat tranfer in vertical channels — a literature survey. By A. Bhattacharyya. 1965. 27 p. Sw. cr. 8:—.
177. Burnout data for flow of boiling water in vertical round ducts, annuli and rod clusters. By K. M. Becker, G. Hernborg, M. Bode and O. Erikson. 1965. 109 p. Sw. cr. 8:—.
178. An analytical and experimental study of burnout conditions in vertical round ducts. By K. M. Becker. 1965. 161 p. Sw. cr. 8:—.
179. Hindered El transitions in Eu^{155} and Tb^{161}. By S. G. Malmskog. 1965. 19 p. Sw. cr. 8:—.
180. Photomultiplier tubes for low level Čerenkov detectors. By O. Strindehag. 1965. 25 p. Sw. cr. 8:—.
181. Studies of the fission integrals of U235 and Pu239 with cadmium and boron filters. By E. Hellstrand. 1965. 32 p. Sw. cr. 8:—.
182. The handling of liquid waste at the research station of Studsvik, Sweden. By S. Lindhe and P. Linder. 1965. 18 p. Sw. cr. 8:—.
183. Mechanical and instrumental experiences from the erection, commissioning and operation of a small pilot plant for development work on aqueous reprocessing of nuclear fuels. By K. Jönsson. 1965. 21 p. Sw. cr. 8:—.
184. Energy dependent removal cross-sections in fast neutron shielding theory. By H. Grönroos. 1965. 75 p. Sw. cr. 8:—.
185. A new method for predicting the penetration and slowing-down of neutrons in reactor shields. By L. Hjärne and M. Leimdörfer. 1965. 21 p. Sw. cr. 8:—.
186. An electron microscope study of the thermal neutron induced loss in high temperature tensile ductility of Nb stabilized austenitic steels. By R. B. Roy. 1965. 15 p. Sw. cr. 8:—.
187. The non-destructive determination of burn-up means of the Pr-144 2.18 MeV gamma activity. By R. S. Forsyth and W. H. Blackadder. 1965. 22 p. Sw. cr. 8:—.
188. Trace elements in human myocardial infarction determined by neutron activation analysis. By P. O. Wester. 1965. 34 p. Sw. cr. 8:—.
189. An electromagnet for precession of the polarization of fast-neutrons. By O. Aspelund, J. Bäckman and G. Trumpy. 1965. 28 p. Sw. cr. 8:—.

Förteckning över publicerade AES-rapparter

1. Analys medelst gamma-spektrametri. Av D. Brune. 1961. 10 s. Kr 6:—.
2. Bestrålningsförändringar och neutronatmosfär i reaktortrycktankar — några synpunkter. Av M. Grounes. 1962. 33 s. Kr 6:—.
3. Studium av sträckgränsen i mjukt stål. Av G. Östberg och R. Attermo. 1963. 17 s. Kr 6:—.
4. Teknisk upphandling inom reaktorområdet. Av Erik Jonson. 1963. 64 s. Kr 8:—.
5. Ågesta Kraftvärmeverk. Sammanställning av tekniska data, beskrivningar m. m. får reaktordelen. Av B. Lilliehöök. 1964. 336 s. Kr 15:—.

Additional copies available at the library of AB Atomenergi, Studsvik, Nyköping, Sweden. Transparent microcards of the reports are obtainable through the International Documentation Center, Tumba, Sweden.

EOS-tryckerierna, Stockholm 1965